BOLETIN DE LA SOCIEDAD ESPAÑOLA DE
Cerámica y Vidrio
www.elsevier.es/bsecv

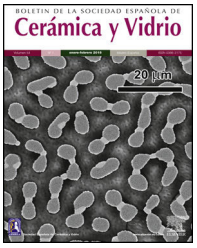

Investigation of the use of nano-titanium dioxide particles synthesized by reflux method as a whitener agent in standard porcelain tiles

Neslihan Tamsu Selli[a,*], *Neslihan Basaran*[a], *Ömer Kesmez*[b]

[a] *Department of Materials Science and Engineering, Gebze Technical University, 41400 Gebze, Kocaeli, Turkey*
[b] *Akdeniz University, Faculty of Science, Department of Chemistry, 07058 Antalya, Turkey*

ARTICLE INFO

Article history:
Received 2 January 2023
Accepted 8 May 2023
Available online 27 May 2023

Keywords:
TiO_2 nanoparticles
Porcelain tile
Whitening agent
Mechanical strength
Optical properties

ABSTRACT

The effects of adding zircon and synthesized TiO_2 nanoparticles (NPs) to standard porcelain tiles on mechanical and optical properties were studied. The obtained TiO_2 nanoparticles had an average particle size of 7.47 nm. The optical properties of TiO_2 NPs were characterized by using UV–visible spectrophotometer. The synthesized TiO_2 NPs and commercial zircon were added to standard porcelain tile composition at a rate of 1%, 2% and 4% by weight. Phase analyzes of the samples were made with XRD, and microstructure analyzes were made with SEM/EDS. Optical dilatometer test was used for sintering studies and densification behaviour was observed with water absorption test. The optical behaviour of the samples was analyzed using spectrophotometric measurements (CIELab method). As a result of this test, it was observed that nano-sized titanium oxide can be used as a whitening agent in porcelain tiles. In addition, the additives made to porcelain tiles also contributed to the increase in mechanical properties.

Investigación del uso de nanopartículas de dióxido de titanio sintetizadas por el método de reflujo como agente blanqueador en gres porcelánico estándar

Palabras clave:
Nanopartículas de TiO_2
Gres porcelánico
Agente blanqueador
Resistencia mecánica
Propiedades ópticas

RESUMEN

Se estudiaron los efectos de añadir circón y nanopartículas (NP) de TiO_2 sintetizadas a baldosas de gres porcelánico estándar sobre las propiedades mecánicas y ópticas. Las nanopartículas de TiO_2 obtenidas tenían un tamaño medio de partícula de 7,47 nm. Las propiedades ópticas de las NP de TiO_2 se caracterizaron utilizando un espectrofotómetro

* *Corresponding author.*
E-mail address: ntamsu@gtu.edu.tr (N. Tamsu Selli).
https://doi.org/10.1016/j.bsecv.2023.05.001

UV-visible. Las NP de TiO_2 sintetizadas y el zircón comercial se agregaron a la composición estándar de baldosas de porcelana a razón de del 1, el 2 y el 4 en peso. Los análisis de fase de las muestras se realizaron con XRD y los análisis de microestructura se realizaron con SEM/EDS. Se utilizó la prueba del dilatómetro óptico para los estudios de sinterización y se observó el comportamiento de densificación con la prueba de absorción de agua. El comportamiento óptico de las muestras se analizó mediante medidas espectrofotométricas (método CIELab). Como resultado de esta prueba, se observó que el óxido de titanio de tamaño nanométrico se puede utilizar como agente blanqueador en gres porcelánico. Además, los aditivos realizados en el gres porcelánico también contribuyeron al aumento de las propiedades mecánicas.

Introduction

The continuous increase in worldwide porcelain tile production capacity and the creation of a competitive environment prompt both manufacturers and researchers to develop production technologies, reduce costs, and provide new functional properties in existing materials [1]. In recent years, the number of studies on alternative raw material sources with cheaper costs in ceramic tile production has increased. Many studies have stated that alternative sources are used instead of zircon, especially in glaze compositions. Romero et al. [2] investigated the crystallization behaviour of zirconia-based glazes. They focused on the effects of phases such as gahnite and diopside formed in these glazes by creating different compositions. In particular, they interpreted the substitution of Fe^{+2} and Ca^{+2} ions for Zn^{+2} in the ferritic crystal structure by XRD analysis. However, it was carried out for the glaze composition. The effect on the whiteness of the samples was not mentioned. Pekkan et al. [3] studied zircon-free opaque frit compositions in single-fired wall tiles glazes. For single-fired wall tiles (K_2O–MgO–CaO–ZnO–Al_2O_3–B_2O_3–SiO_2), system compositions were prepared. The study observed that diopside and wollastonite phases were formed without the need for a nucleation agent. New compositions were prepared by completely removing zircon from the single firing frit composition and changing the CaO/MgO and Al_2O_3/alkali ratios in the frit composition. The opacity provided by zircon was obtained with the diopside and wollastonite phases. However, this study is also a study on frit compositions. Sun et al. [4] conducted opacification studies in glaze compositions in their studies. They used TiO_2 as the opacifier. They tried to prevent the glaze yellowing tendency of TiO_2 with the materials they added to the composition. Gajek et al. [5] examined white glazes with the gahnite phase in their study. Glaze compositions were prepared in the (ZnO–R_2O–RO–Al_2O_3–SiO_2) system. In particular, they stated that the opacity of the glaze increased with the increase of the recipe gahnite phase. Tarhan [6] increased the whiteness of the body by creating diopside and anorthite phases in the porcelain tile. This study investigated the effects of diopside and anorthite phases on whiteness by using diopside frit and bentonite raw materials in the body. However, in this study, zircon was not eliminated but also included in the composition. By creating anorthite phases in the body, the effect of whiteness on porcelain bodies has been investigated in the literature. Selli [7] investigated the whitening effect in porcelain tile by forming an anorthite phase in the porcelain tile structure in study. Taskiran et al. [8] investigated the whiteness effect on porcelain bodies by creating anorthite phases. In addition to these, more environmentally friendly products are created using waste materials, especially with the efforts to reduce energy costs. Güngör et al. [9] reported the effects of zinc oxide by using galvanized waste in sanitary ware. They stated that zinc oxide forms the gahnite ($ZnAl_2O_4$) phase in the body. Zinc oxide reduced the sintering temperature of the ceramic sanitary ware material body. They also emphasized that it does not harm body colour.

As can be seen, the studies in the literature are generally focused on the glaze, and the studies on the ceramic body are very few. In the studies on the body, commercial zirconium silicate was generally used again, and it was not removed from the final compositions obtained. Studies conducted in the body also focused on a kind of micro-sized raw materials usage. High purity imported starting powders (such as CaO and Al_2O_3) were used as raw materials in the newly formed crystals. Unlike previous studies, this study aimed to disperse nano-sized titanium oxide powder with a high refractive index in the microstructure and increase the whiteness of the ceramic tile body. Nano titanium oxide powders were synthesized by sol–gel method and then added to porcelain tile bodies.

Experimental

Synthesis of the nano-sized TiO_2 powder

TiO_2 nanoparticle was synthesized by reflux method according to our previously reported method [10–12]. Briefly, $Ti[OCH(CH_3)_2]_4$ and 1-Propanol were weighted and the obtained solution was stirred until a clear and homogeneous solution was formed. $Ti(OPr)_4/H_2O$ and $Ti(OPr)_4$/HCl mol/mol ratios were 3.60 and 1.96, respectively. HCl was added dropwise into alkoxide solution at a rate of 1 ml min^{-1} and stirring the solution for 5 min at ambient temperature. After stirring for 5 min, water was added to the final solution at the same rate. The mixture was stirred at ambient temperature for 10 min. The final solution was taken into a reflux system and the

reaction was conducted at 100 °C in an oil bath for 20 h. The obtained nanoparticles were separated by centrifuging.

Preparation of the samples

In this study, nano-sized TiO_2 powder was prepared to add the standard porcelain tile composition. Chemical characterization was carried out by means of wavelength dispersive X-ray fluorescence spectrometry (XRF), using Philips Model PW 2400 XRF Instrument fitted with an Rh white fluorescent tube. The sample was prepared as fused beads using a Philips PERL'X3 instrument.

The raw materials weighed over 100 g and were ground in ball jet mills with a 1.5–2% sieve residue over 45 μm at the determined ratios. Mill pot are made of alumina and has a volume of 500 ml. Wet milling was done using 75 ml of water. Alumina balls with a diameter of 30 mm in the amount of 125 grams and with a diameter of 20 mm in the amount of 75 g were used. The ratio of ball to material is 2/1. No dispersing agent used. Approximately 60% solid ratio was applied. After this stage, commercial zirconium silicate ($ZrSiO_4$) and nano-sized titanium oxide (TiO_2) powders were added to the standard porcelain slurry at a rate of 1%, 2%, and 4% by weight. The chemical composition of commercial zirconium silicate is 31 wt% SiO_2, 66% ZrO_2. It also contains trace amounts of Al_2O_3. High aesthetic properties as well as strength are the desired features in ceramic tiles. Zircon is important material for the production of white ceramic tiles. The volume of zircon sand (zirconium silicate) used in the ceramic tile industry covers approximately 55% of the world's zircon sand production [13]. Zircon is included in the body due to its whitening feature. Nano TiO_2 is expected to both whiten the body like zircon and increase the mechanical properties more than zircon.

Zircon and TiO_2 NPs were dispersed into the slurry with the help of Heidolp RZR 2020 brand mechanical mixer. Then, the slurry dried at 100 °C for 24 h. For granulation of the dried powders, they were moistened by spraying 10% wt water on them. Formed granules were passed through sieves with aperture sizes of 600 and 250 μm to collect between them. The weighed granules powders were put into the cavity of a steel die and shaped by applying a pressure of 30 MPa by using a hydraulic press. The rectangular-shaped samples were prepared for the mechanical study. The discs' dimensions were 31.5 mm in diameter, and rectangular bars were 75 mm × 7 mm × 5 mm. Samples were fired at 1220 °C for 30 minutes in laboratory furnace (Nabertherm Furnace). Fig. 1 shows the illustration of the experimental procedure for nano-size titanium oxide powders. Sample numbers and details are summarized in Table 1.

Water absorption value of the samples was determined by water saturation under vacuum and Archimedes' principle (ISO 10545-3) by using related Eq. (1) [14,15].

$$\%\,\text{Water absorption (wa)} = \left[\frac{(ww - wd)}{wd}\right] \times 100 \quad (1)$$

where wd, dry weight of the sample, ww, wet weight of the sample, wa, weight of solid suspended in water.

Table 1 – Samples and details.

Samples	Details
STD	Standard porcelain tile body slurry.
STD + %1 ZS	Standard porcelain tile slurry with 1% by weight zirconium silicate added
STD + %2 ZS	Standard porcelain tile slurry with 2% by weight zirconium silicate added
STD + %4 ZS	Standard porcelain tile slurry with 4% by weight zirconium silicate added
STD + %1 TiO_2	Standard porcelain tile slurry with 1% by weight titanium oxide added
STD + %2 TiO_2	Standard porcelain tile slurry with 2% by weight titanium oxide added
STD + %4 TiO_2	Standard porcelain tile slurry with 4% by weight titanium oxide added

Firing shrinkage value of the samples was calculated by using Eq. (2) [16].

$$\%\,\text{Firing shrinkage} = \left[\frac{(LB - LD)}{LB}\right] \times 100 \quad (2)$$

where LB, dry dimension of the sample, LD, fired dimension of the sample.

The colour values of the new compositions and standard composition were measured by a spectrometer (Minolta CR, 300 Colorimeter). The colorimeter operates on the CIELab method, which is utilized technique in the ceramic production to determine the whiteness and colour of the tiles by measuring three main parameters (Hunter parameters) L^* (brightness) from absolute white $L = 100$ to absolute black $L = 0$, an (red–green), bn (yellow–blue) elaborated from the visible spectra [17].

The illuminant was visible light for determining the colour determination procedure, and the incident angle was 90°. Five measurements were made for each sample.

Characterization of the samples

Characterization of the TiO_2 NPs

A Rigaku 2200 D Max X-ray diffractometer (XRD) with Cu Ka radiation ($k = 0.154$ nm) in the range of 5–80°, at 40 kV and 40 mA conditions was used in order to determine the crystal phases of the TiO_2 NPs. UV–Vis–NIR spectrophotometer was used to investigate the optical properties of the TiO_2 NPs. The UV–vis diffuse reflection absorption spectra of samples were recorded three times by a Varian Cary 5000 UV–VIS–NIR spectrophotometer with a diffuse reflectance accessory (DRA-2500) in diffuse reflectance mode and in the wavelength range from 200 to 800 nm. All samples were heat-treated at 60 °C 24 h under vacuum prior to acquisition of the UV–Vis spectra and the XRD analysis. The particle size distribution of TiO_2 NPs was determined by a particle size analyser (Zetasizer Nano-ZS, Malvern Instruments). The particle size analysis is performed according to dynamic light scattering principle and the particle size range of the device is specified as 0.6 nm–6 μm. The synthesized TiO_2 powders were dispersed ultrasonically in deionized water without using a dispersant, prior to acquisition of the particle size distribution analysis. Finally, transparent TiO_2 sols were obtained.

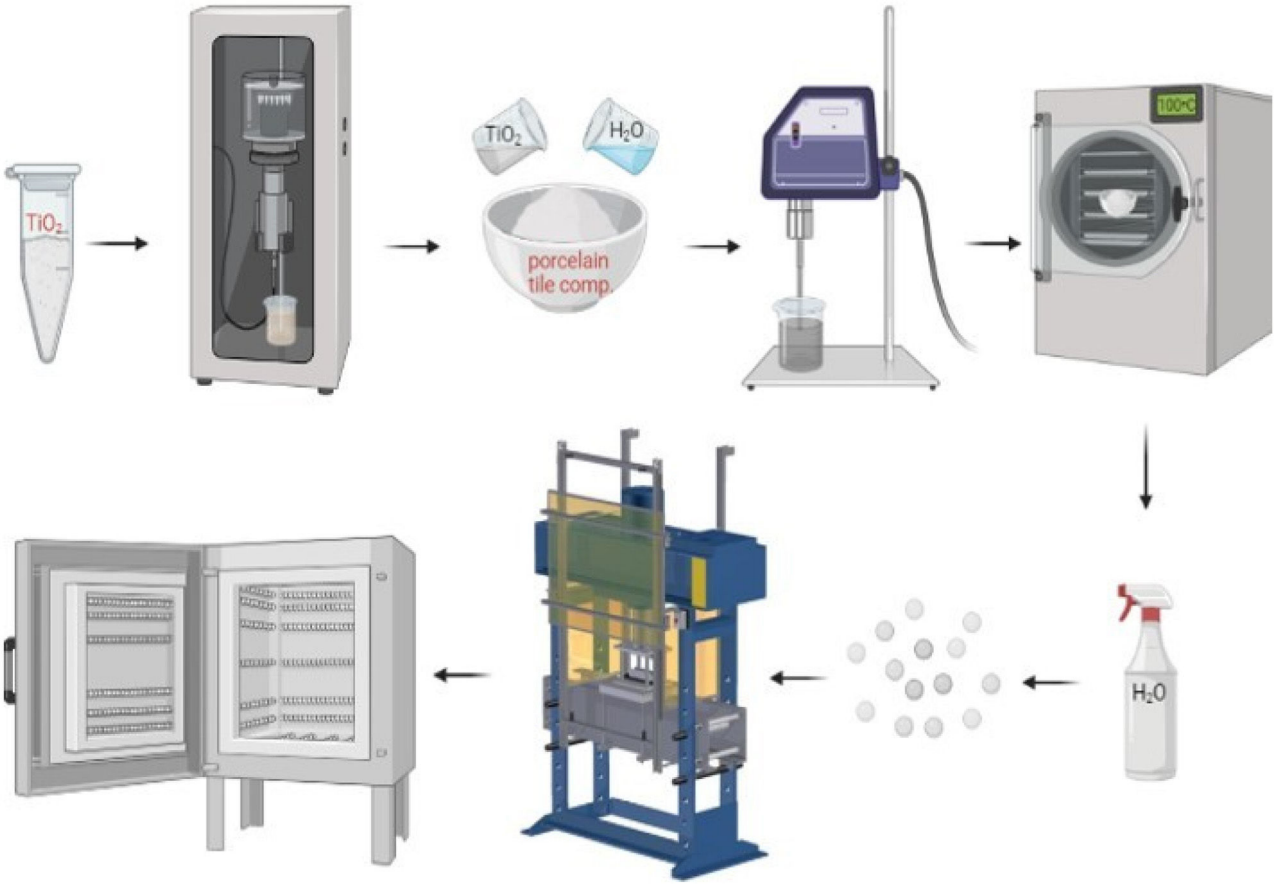

Fig. 1 – Illustration of the experimental procedure in this study starting from the nano-sized titanium oxide powders were added to the standard porcelain slurry to the firing process.

Determination of the sintering behaviour of the samples
Sintering temperatures of the compositions were determined by flex point (i.e., temperature at which densification rate is maximum) analyses as stated by Paganelli [18] using the optical dilatometer (Misura 3.32, ODHT-HSM, Expert System Solutions, Italy). The derivative of the sintering curve (dy/dT) obtained as a result of the optical dilatometer is called the "flex point" temperature, which corresponds to the maximum expansion amount and the fastest sintering. The rod-shaped samples with a diameter of 15 mm, specially prepared for the optical dilatometer device, were heat treated up to 1250 °C at a speed of 10 °C/min.

Flexural strength of the samples
The flexural strength of green and sintered samples was measured by three-point bending test using an electronic universal tester (Model 5569, Instron Ltd.). Rod-shaped samples were used for the test and 8 samples were used for each composition. Tests were carried out according to ASTM C1161-90 standard with a lower span of 50 mm and crosshead speed of 1 mm/min [19].

X-ray diffraction analysis
X-ray diffraction (XRD) method was applied to detect the crystalline phases formed in the microstructure of sintered samples. In the analyses, the samples were used in powder form. They were scanned at 2°/min speed in the range of 5–70° with CuKα radiation, (λ = 0.154 nm), at 40 kV and 40 mA conditions using RIGAKU 2200 DMAX diffractometer.

Scanning electron microscopy analysis
The microstructures of the samples were examined by scanning electron microscopy (SEM) analysis with the use of Philips XL30-SFEG-SEM equipped with energy dispersive X-ray analysis (EDX). Firstly, the surface of the samples was made suitable for SEM analysis by grinding with a series of SiC abrasive papers and then polished using diamond paste. The polished surfaces were chemically etched in an aqueous solution containing 3% HF for about 2 min to reveal the crystalline structure, then the sample surfaces were coated with gold.

Results and discussion

TiO_2 NPs

The peaks in the XRD pattern (Fig. 2) demonstrated that TiO_2 with 00-021-1272 card number exists in the sample.

It was found that all the sharp peaks observed at 25.060°, 37.540°, 47.759°, 54.121°, 62.142°, 70.056° and 75.019°. 2 theta values of the diffraction planes of (101), (004), (200), (105), (204), (220) and (215) were detected [20,21]. The obtained results

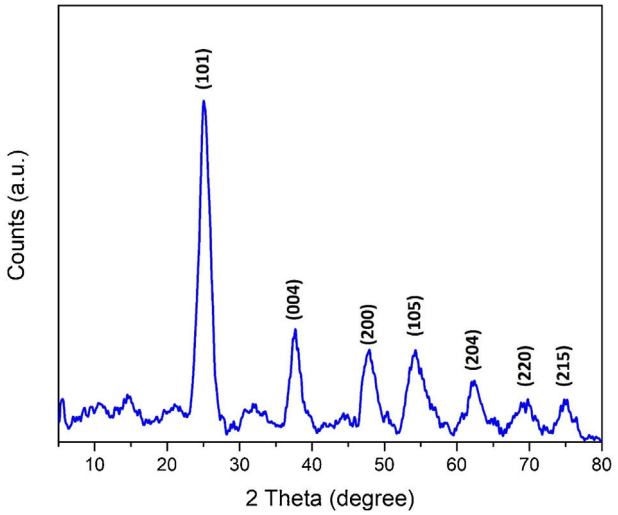

Fig. 2 – XRD pattern of TiO_2-NPs.

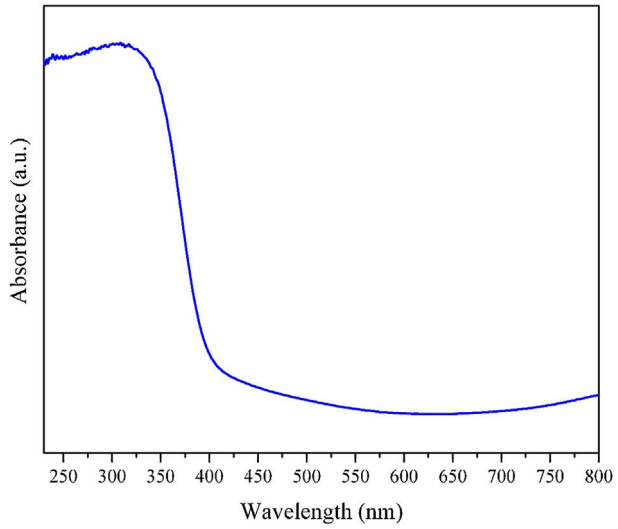

Fig. 3 – UV–vis spectra of TiO_2 NPs.

with narrow and sharp peaks are the signs of well-developed anatase TiO_2 (JCPDS#21-1272) reported in the literature [11,12].

The optical properties of TiO_2 NPs were characterized by using UV–visible spectrophotometer. The UV-DRS reflection peak for TiO_2 NPs was observed at 200–800 nm, as shown in Fig. 3.

It can be observed that TiO_2-NPs has a strong absorption band at about 410 nm which is corresponding to TiO_2 band gap excitation. According to the UV–visible spectrometer analysis, the obtained result indicates that the synthesized particles were photosensitive in UV region. Dynamic light scattering is a widely used technique for the determination of particle size. Particle size distribution of TiO_2 NPs was determined by a particle size analyzer (Zetasizer Nano-ZS, Malvern Instruments).

The obtained TiO_2 NPs had an average particle size of 7.47 nm and presented a monosize distribution which is presented in Fig. 4.

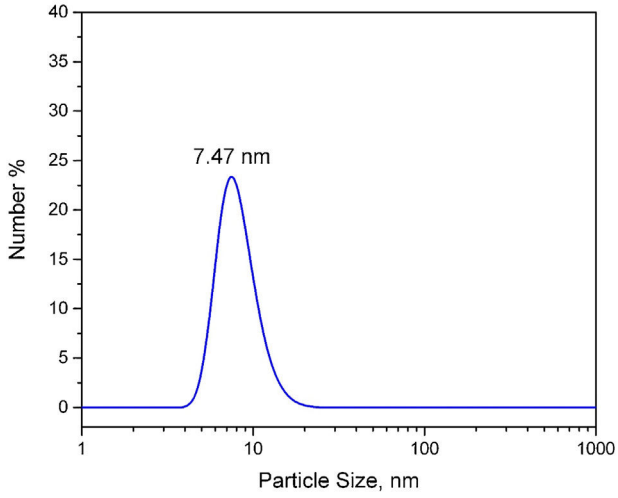

Fig. 4 – The size distribution of TiO_2 NPs by number.

Table 2 – Chemical composition of the standard porcelain tile body (STD).

Compounds	STD (wt.%) ± sd[a]
SiO_2	66.70 ± 2.00
Al_2O_3	16.80 ± 2.00
Fe_2O_3	0.10 ± 0.02
CaO	2.50 ± 0.10
MgO	0.70 ± 0.10
Na_2O	3.30 ± 0.10
K_2O	0.80 ± 0.10
L.O.I.[b]	9.10 ± 1.00

[a] sd: standard deviation.
[b] L.O.I: loss of ignition.

Sintering behaviour of the samples

The sintering temperatures of commercial zirconium silicate and nanosized titanium oxide added samples are presented in Fig. 5. The flex point of standard porcelain tile is 1220 ± 2 °C. This temperature decreased to 1219 ± 2 °C with the addition of 1% zirconium silicate to the standard porcelain tile, to 1215 ± 2 °C with 2% zirconium silicate, and finally to 1210 ± 2 °C with the addition of 4% zirconium silicate. On the other hand, with the addition of nanosized titanium oxide, there was a severe decrease in the flex point of the porcelain tile. This point decreased to 1065 ± 2 °C, addition of 1% TiO_2, to 1040 ± 2 °C with the addition of 2% TiO_2, and 1036 ± 2 °C with the addition of 4% TiO_2. This can be explained by increasing the sintering kinetics of nanosized particles. Hussein et al. reported that sintering of nanocrystalline particles leads to lower sintering temperatures and faster processing times [22].

Phases and microstructural analyses

Chemical analysis of the standard wall tile body composition (denoted as STD) is given in Table 2.

In the study, phase analysis of the standard porcelain tile, which did not add any whitening agent, was performed. The

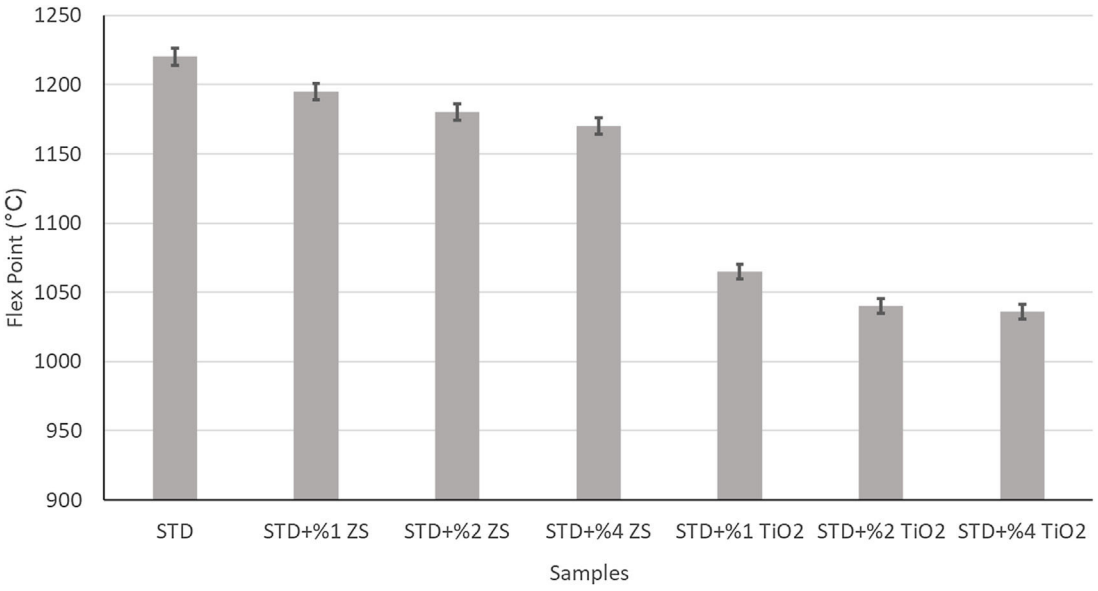

Fig. 5 – Flex points of the samples.

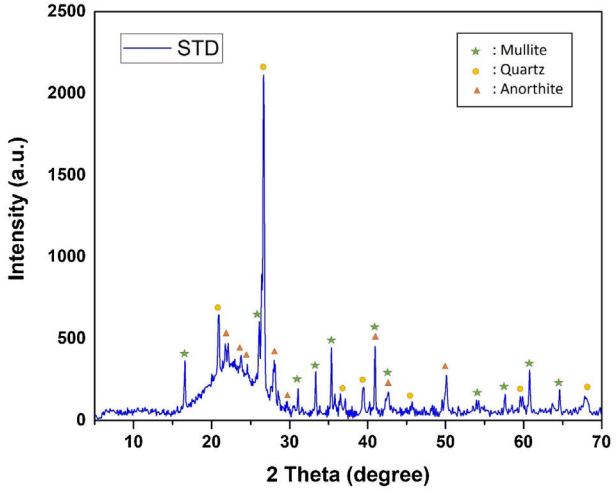

Fig. 6 – XRD analysis of the standard porcelain tile.

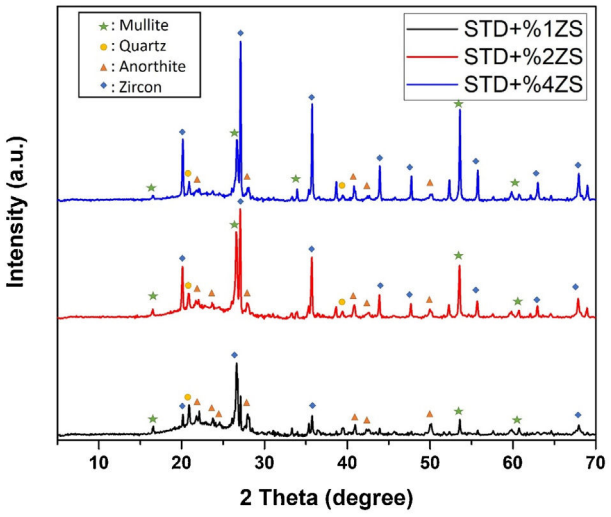

Fig. 7 – XRD analysis of the ZS added compositions.

XRD graph of the standard porcelain tile is given in Fig. 6. According to this graph, the phases contained in the porcelain tile are quartz (JCPDS#46-1045), anorthite (JCPDS#41-1486) and mullite (JCPDS#15-0776).

XRD analyzes of the whitening agent added compositions were also performed (Fig. 7). For zirconium silicate addition, there are zircon (JCPDS#7-3430), mullite (JCPDS#15-0776), anorthite (JCPDS#41-1486) and quartz (JCPDS#46-1045) phases in porcelain tile body. With the increase in the amount of zirconium silicate, there is an increase in the peak intensity of the formed zirconia phase.

In the nanoscale titanium oxide addition, the phases formed are mullite (JCPDS#15-0776), quartz (JCPDS#46-1045), anorthite (JCPDS#41-1486) and rutile (JCPDS#21-1276). As the titanium oxide ratio increased, the intensity of the rutile peak increased [23] (Fig. 8).

Microstructure and EDX analyzes of the prepared compositions were also performed. The microstructure of the standard porcelain tile and the result of the EDX analysis made from the image are given in Fig. 9. In the EDX analysis, it was determined that the rod-like grains were mullite (M) (Fig. 9b), the angular grains were quartz (Q) (Fig. 9c) and the round grains were anorthite (A) (Fig. 9d).

The microstructures and EDX analysis of the samples obtained by adding 1, 2, and 4 wt% zirconium silicate within the porcelain tile are given in Fig. 10. It is seen that especially the white-coloured grains are zirconium silicate. It has been determined that needle-like grains are mullite and angular grains are quartz.

The microstructure images and EDX analysis of the titanium oxide added samples are presented in Fig. 11. Similar to the standard, these microstructures also contain mullite (M),

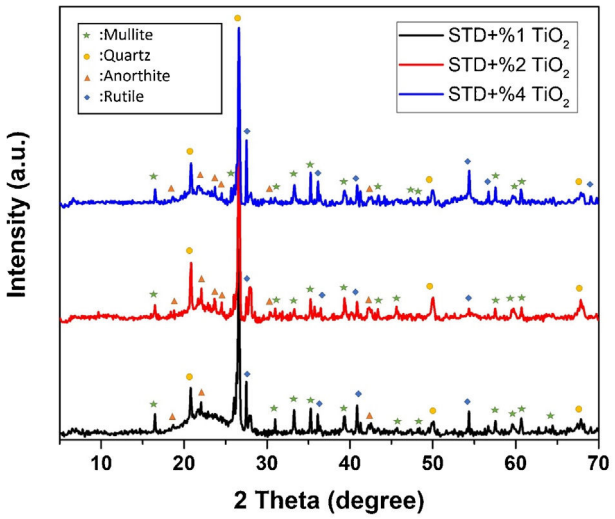

Fig. 8 – XRD analysis of the TiO_2 added compositions.

anorthite (A), and quartz (Q) crystals. EDX analyzes were performed on the rectangular prism-shaped rod-like crystals, and the titanium peak predominates. This result shows that these are rutile (R) crystals, consistent with the XRD analysis result.

Rutile crystals were formed in the standard porcelain tile microstructure with the addition of titanium oxide NPs. In order to examine these crystals in more detail, their microstructures at higher magnifications are presented in Fig. 12. The crystal sizes of rutile crystals varying between 150 and 200 nm were formed.

Surface microstructures of the samples were also analyzed. The microstructure image of the standard porcelain tile is given in Fig. 13. In the traditional porcelain tile microstructure, there may be large pores with dimensions of 90–100 μm, as well as tiny pores with a diameter of 5–10 μm.

The microstructure images taken from the surface of the whitening agent added compositions are given in Fig. 14. It is seen that there are large pores up to 80–90 μm in the microstructure obtained by adding 1% by weight of zirconium silicate. When the contribution ratio is increased to 2 percent, it is seen that the pores are slightly smaller in size, and there is no interaction (clustered pores) with each other. With the addition of 4 weight percent zirconium silicate, it is seen that the pores become more spherical and decrease in size (pores up to a maximum of 50 μm). The microstructure images obtained by adding nano-sized titanium oxide to the porcelain body are given in Fig. 14d–f. With the addition of 1% by weight of titanium oxide, the pore sizes reached a maximum of 80 μm. It can be said that with the addition of 2% by weight of titanium oxide, the pores become smaller, spherical and their amount decreases. The maximum pore size is about 30 μm. Completely spherical pores were formed with 4% titanium oxide by weight. The maximum pore size is approximately 20 μm. The amount of pores has also decreased considerably.

Technological properties of the samples

This study, first, examined the technical properties of the standard porcelain tile represented in Table 3. Then, water absorption, and colour values of all the studied compositions were evaluated. The water absorption value of standard porcelain tile is % 0.065 ± 0.01, and colour values are L^*: 72.01, a^*: 5.77, b^* value is 15.17. With the addition of zirconium silicate to standard porcelain tiles, there is an increase in L^* value and a decrease in a^* and b^* values. Especially with the addition of zirconium silicate at the maximum rate (4% by weight), the increase in L^* value reached its maximum (83.20 ± 0.01). On the other hand, the addition of nano-sized titanium oxide caused

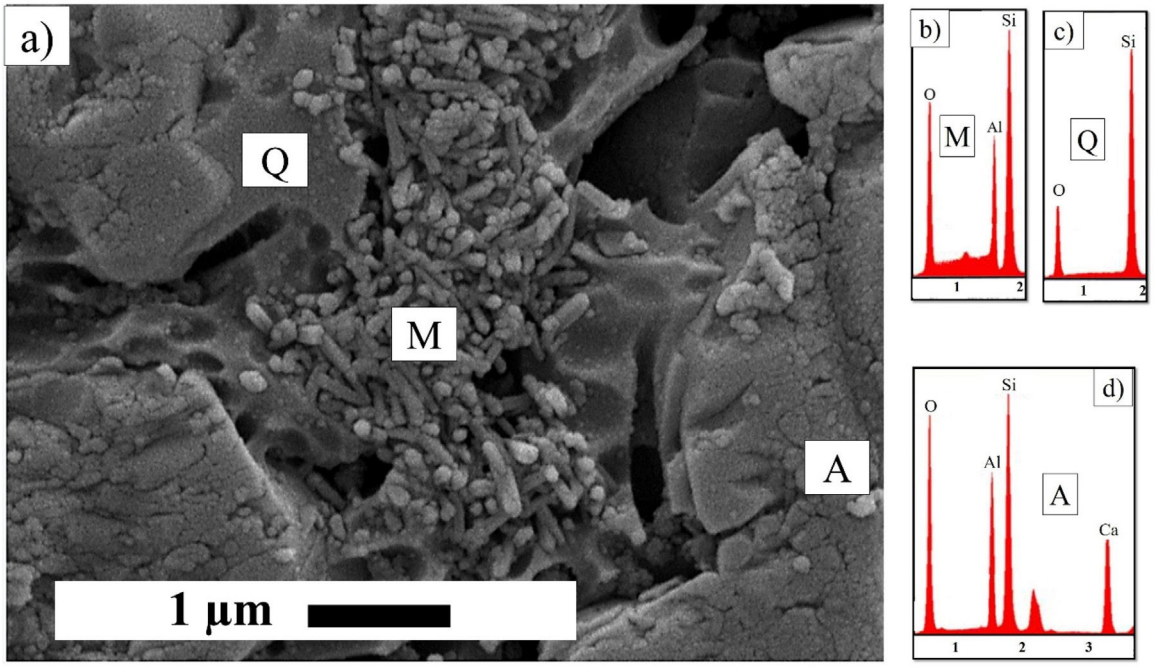

Fig. 9 – (a) Microstructure of standard porcelain tile and EDX analysis of (b) mullite, (c) quartz and (d) anorthite.

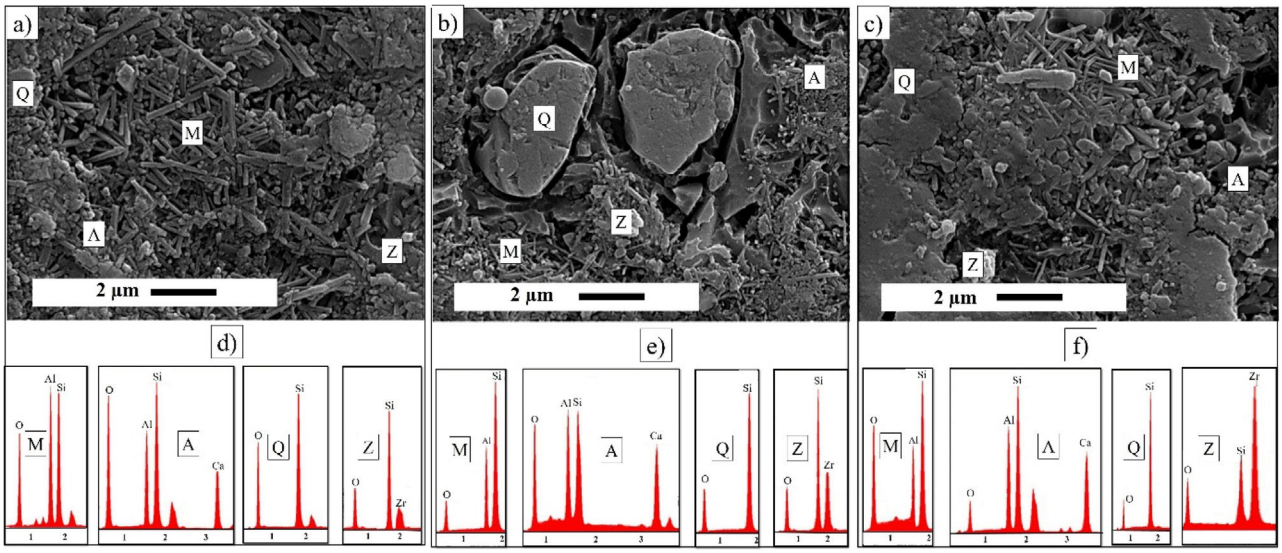

Fig. 10 – Microstructure of (a) STD + %1ZS, (b) STD + %2ZS, (c) STD + %4ZS and EDX analysis of (d) STD + %1ZS, (e) STD + %2ZS, (f) STD + %4ZS.

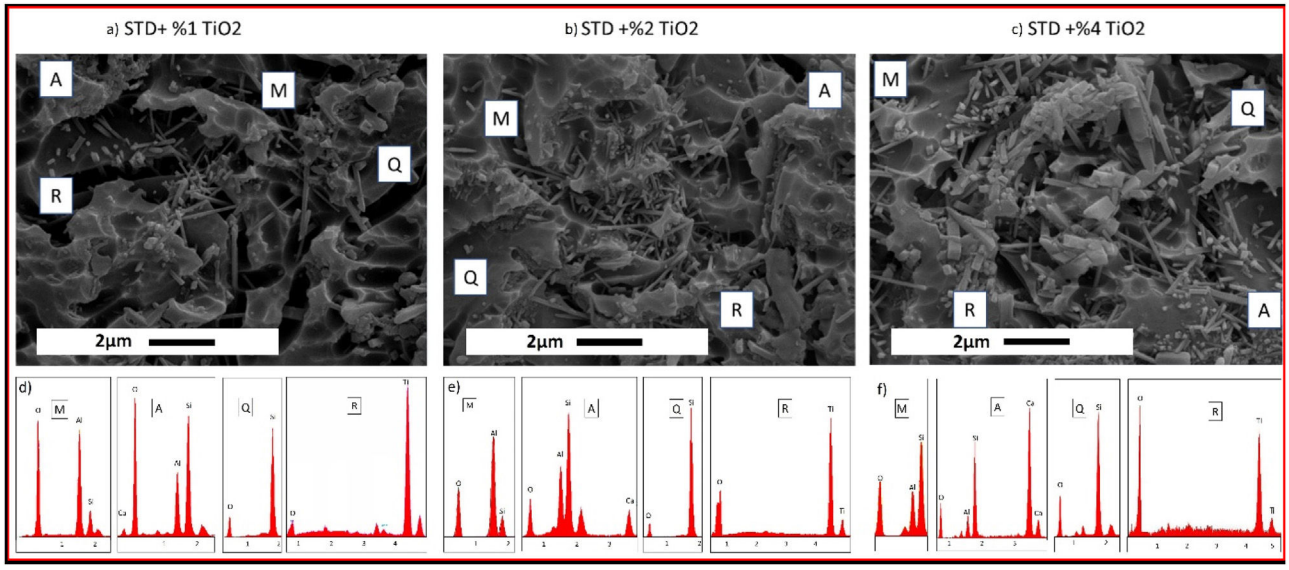

Fig. 11 – Microstructure of (a) STD + %1TiO_2, (b) STD + %2TiO_2, (c) STD + %4TiO_2 EDX analysis of (d) STD + %1 TiO_2, (e) STD + %2 TiO_2, (f) STD + %4 TiO_2.

Table 3 – Technological properties of the samples fired at 1200 °C for 30 min.

Sample	Water absorption	Colour value			Firing shrinkage (%) ± SD[a]
	(%) ± SD[a]	L^* ± SD[a]	a^* ± SD[a]	b^* ± SD[a]	
STD	0.065 ± 0.01	72.01 ± 0.3	5.77	15.17	7.1 ± 0.1
STD + %1 ZS	0.059 ± 0.15	75.07 ± 0.2	3.88	10.14	7.2 ± 0.07
STD + %2 ZS	0.055 ± 0.02	81.22 ± 0.15	1.46	9.92	7.5 ± 0.084
STD + %4 ZS	0.048 ± 0.005	83.20 ± 0.01	1.27	9.83	7.8 ± 0.03
STD + %1 TiO_2	0.045 ± 0.017	76.82 ± 0.18	2.75	9.98	7.4 ± 0.017
STD + %2 TiO_2	0.032 ± 0.006	83.26 ± 0.25	1.09	8.79	7.7 ± 0.09
STD + %4 TiO_2	0.011 ± 0.003	85.38 ± 0.16	0.61	8.02	8.3 ± 0.01

[a] SD: standard deviation.

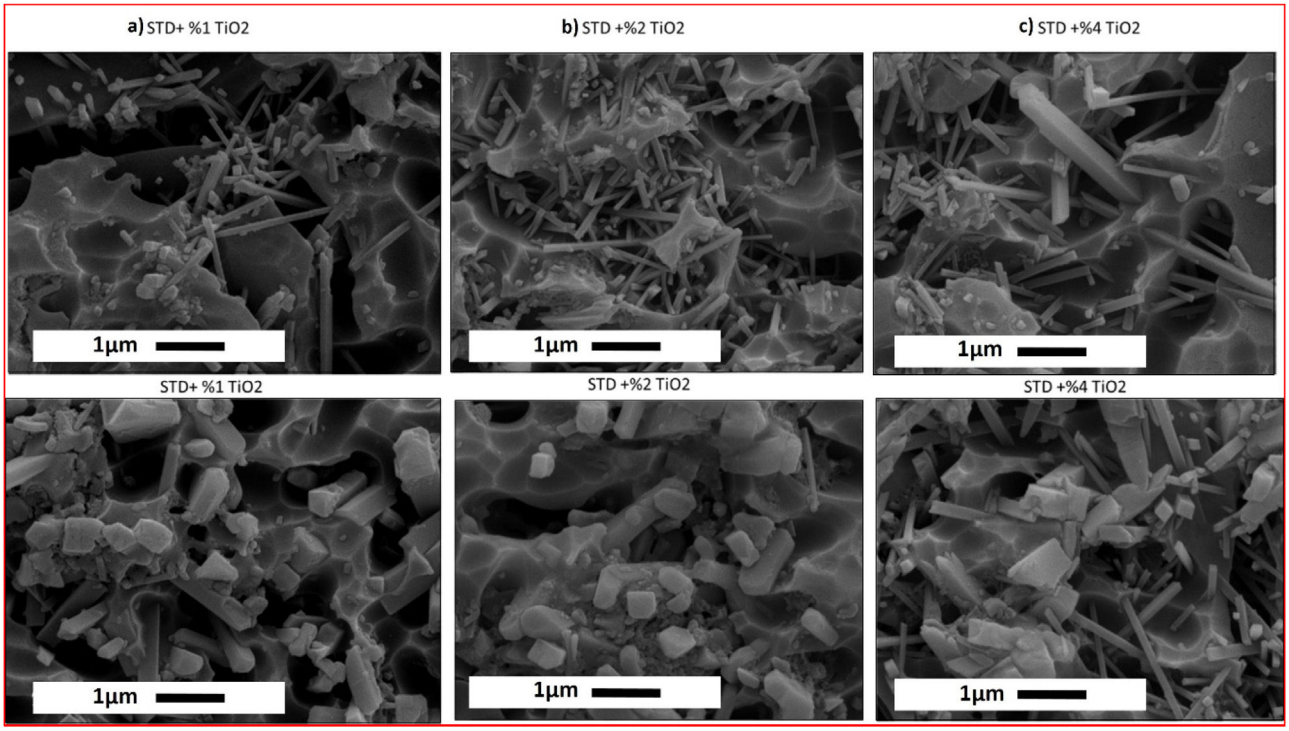

Fig. 12 – Microstructure analysis of rutile crystals for (a) STD + %1TiO_2, (b) STD + %2TiO_2, (c) STD + %4TiO_2.

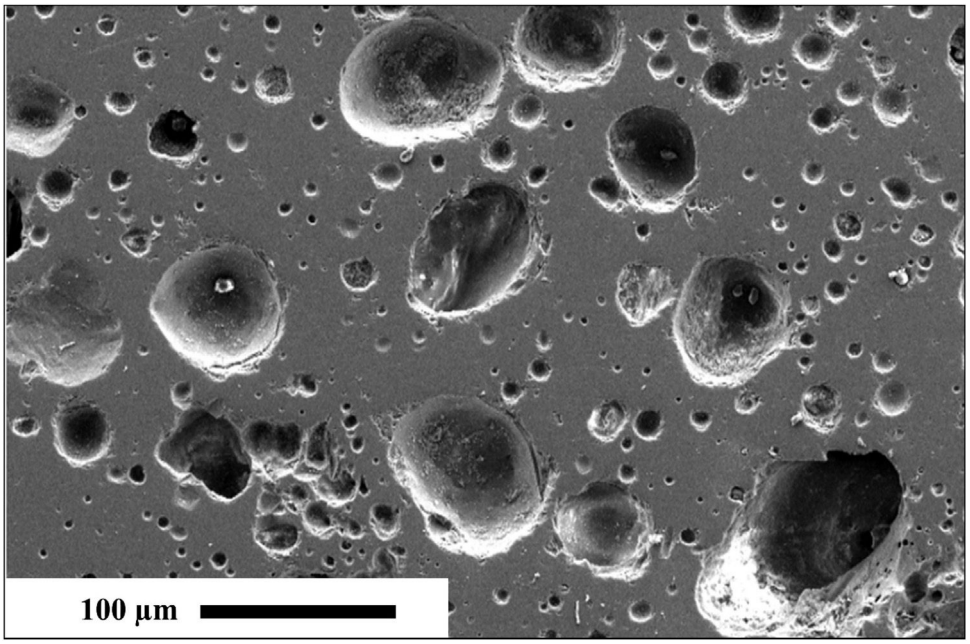

Fig. 13 – Microstructure image of standard porcelain tile.

a higher increase in L^* value in all additive ratios compared to zirconium silicate. With the addition of nano-sized titanium oxide at the maximum rate, the L^* value reached 85.38 ± 0.16.

With increasing additive ratio, L^* values increased, a^* and b^* values decreased. As L^* increases, the hues become more vivid, indicating light intensity. A higher value of the L^* parameter indicates a greater tendency towards white [17]. In addition to technical features, appearance and body whiteness are very important for porcelain tiles. For the white floor, zircon, which acts as a whitening agent in porcelain tiles, is added. In this study, TiO_2 also served the same role and contributed to the production of an aesthetic quality porcelain tile [7]. The tableted and fired forms of the standard porcelain tiles with and without additions are presented in Fig. 15.

The positive a^* number is associated with red/magenta. A decrease in this value means that the redness in the sample

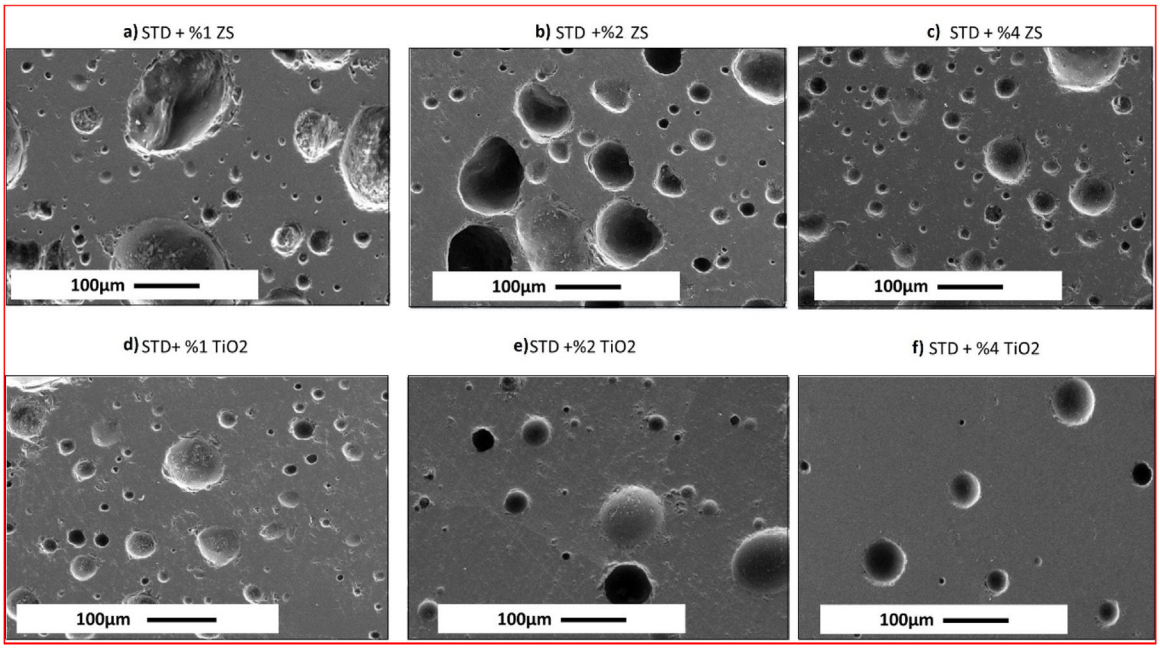

Fig. 14 – Microstructure image of (a) STD + %1ZS, (b) STD + %2ZS, (c) STD + %4ZS, (d) STD + %1TiO_2, (e) STD + %2TiO_2, (f) STD + %4TiO_2.

Fig. 15 – Views of standard porcelain tiles with and without additions.

is reduced. A high b^* value that is positive corresponds to yellow. A decrease in this value means that the yellowness in the sample is reduced [24].

The technological properties of the compositions obtained by adding commercial zirconium silicate and synthesized nano-sized titantium oxide to standard porcelain tile slurry are given in Table 3. Water absorption value decreased to 0.059% the addition of 1% weight of zirconium silicate to the standard porcelain tile, 0.055% with the addition of 2%, and to 0.048% the addition of 4%. With the additions made by firing shrinkage (1%, 2% and 4% by weight), the values reached 7.2%, 7.5% and 7.8%, respectively.

The water absorption values obtained with nano-sized titanium oxide are lower than zirconium silicate. This value decreased to 0.045% with the addition of 1% titanium oxide by weight, 0.032% water absorption with the addition of 2% titanium oxide by weight, 0.011% water absorption with the addition of 4% titanium oxide by weight. The firing shrinkage values obtained with nano-sized titanium oxide are higher than zirconium silicate. When the firing shrinkage values are examined, 7.4% firing shrinkage value is obtained with the addition of 1% titanium oxide by weight, 7.7% with the addition of 2% oxide, and finally 8.3% with the addition of 4% titanium oxide.

Table 4 – Mechanical strength values of the samples.

Sample	Mechanical strength values (MPa) ± SD[a]
STD	36.20 ± 0.10
STD + %1 ZS	36.50 ± 0.02
STD + %2 ZS	36.80 ± 0.15
STD + %4 ZS	37.10 ± 0.055
STD + %1TiO_2	36.40 ± 0.01
STD + %2TiO_2	37.00 ± 0.048
STD + %4TiO_2	38.40 ± 0.03

[a] SD: standard deviation.

Mechanical properties of the samples

Mechanical strength tests were carried out to examine whether zirconium silicate and nano-sized titanium oxide, which will create a whitening effect on porcelain tiles, impact mechanical properties. The strength values of the samples are presented in Table 4. According to ISO-10545 standards, the mechanical strength value of porcelain tiles is required to be higher than 35 MPa ± 0.10. It is seen that it provides the standard deal with the addition of whitening agent. With the addition of zirconium silicate, the mechanical

strength of the porcelain tile increased from 36.20 MPa ± 0.10 to 37.10 MPa ± 0.055 with the addition of nano-sized TiO_2, the strength value of the standard porcelain tile increased to a maximum of 38.40 MPa ± 0.03. Yang et al. observed an increase in flexural strength when nano-leucite was added to a porcelain matrix [25]. This was attributed to a dispersion enhancement phenomenon, which is achieved when the NPs are homogeneously dispersed in the glassy matrix, allowing for such performance improvements [21]. Belnou et al. observed that the bending strength doubled when they added nanosized alumina to porcelain [26]. Bakhtierkhalzi et al., in their study examining the effect of TiO_2 on ceramic composites, reported that mechanical properties were improved with the addition of TiO_2 [27]. Zhang et al. reported that the Vickers hardness of $MgO–Al_2O_3–SiO_2$ glasses increased with the increase in TiO_2 content for the same heat treatment [28]. In the study of Hsien-Nan Kuo et al. with bioceramics, mechanical properties improved with increasing TiO_2 addition [29].

Conclusions

When the effects of zircon and TiO_2 NPs additives made on standard porcelain tiles on the sintering behaviour were examined, it was observed that the flex point decreased with increasing additive amount. The TiO_2 NPs additive caused a great decrease in the flex point than zircon. The low sintering temperature achieved to decrease the production cost. In addition, reducing energy consumption shows the environmental contribution of this study.

The strength of porcelain tiles showed a gradual increase as nano-TiO_2 addition increased. STD + 4%TiO_2 sample containing 4.0% nano-TiO_2 by weight reached its maximum strength value (38.40 ± 0.10). This increase was not observed in porcelain tiles containing the same amount of zircon. The improvement of mechanical properties with the addition of nano TiO_2 can be explained by mechanical strengthening mechanisms. SEM images and XRD results confirm that agglomerated rutile crystals increase as the nano-TiO_2 ratio increases. Titanium dioxide dispersed in the glassy matrix acts as a strong barrier, causing the crack to deviate if a load is applied to the sample.

In addition, it was determined that the water absorption values decreased with the increasing amount of TiO_2 NPs. These values were also supported by microstructure images. The open pores decreased visibly with increasing additive ratio and the sample get more densified. When compared with zircon, it has been determined that there are large and deep pores in zircon added porcelains at the same additive ratio. This is proof of why water absorption values are lower in titanium oxide added samples.

The appearance, whiteness and aesthetic quality of porcelain tiles are as important as their technical features. It has been determined by the colour measurement tests that the colours of the samples change to lighter tones as desired with the increasing amount of additives. This result showed that TiO_2 NPs can be used as a whitening agent in porcelain tiles.

Conflict of interest

The authors declare that they have no known competing financial interest or personal relationship that could have appeared to influence the work reported in this paper.

REFERENCES

[1] N. Tangboriboon, S. Pornsimma, A. Sirivat, Embedding eggshell as flux in porcelain clay products to reduce firing temperature via extrusion process, Middle East J. Sci. Res. 24 (2016), http://dx.doi.org/10.5829/idosi.mejsr.2016.24.05.23462.

[2] M. Romero, J.M. Rincón, A. Acosta, Crystallisation of a zirconium-based glaze for ceramic tile coatings, J. Eur. Ceram. Soc. 23 (2003) 1629–1635, http://dx.doi.org/10.1016/S0955-2219(02)00415-6.

[3] K. Pekkan, B. Karasu, Zircon-free frits suitable for single fast-firing opaque wall tile glazes and their industrial productions, J. Eur. Ceram. Soc. 29 (2009) 1571–1578, http://dx.doi.org/10.1016/j.jeurceramsoc.2008.10.010.

[4] S. Sun, H. Ding, A. Weihua, Y. Liu, L. Chang, J. Zhang, Preparation of a $CaCO_3–TiO_2$ composite based opaque glaze: Insight into the mechanism of opacification and glaze yellowing inhibition, J. Eur. Ceram. Soc. 40 (2020), http://dx.doi.org/10.1016/j.jeurceramsoc.2020.07.063.

[5] M. Gajek, J. Partyka, M. Leśniak, A. Rapacz-Kmita, Ł. Wójcik, Gahnite white colour glazes in $ZnO–R_2O–RO–Al_2O_3–SiO_2$ system, Ceram. Int. 44 (2018), http://dx.doi.org/10.1016/j.ceramint.2018.05.265.

[6] M. Tarhan, Whiteness improvement of porcelain tiles incorporated with anorthite and diopside phases, J. Therm. Anal. Calorim. 138 (2019), http://dx.doi.org/10.1007/s10973-019-08268-8.

[7] N. Tamsu Selli, Development of anorthite based white porcelain stoneware tile compositions, Ceram. Int. 41 (2015) 7790–7795, http://dx.doi.org/10.1016/j.ceramint.2015.02.112.

[8] M. Taskiran, N. Demirkol, A. Capoglu, A new porcelainised stoneware material based on anorthite, J. Eur. Ceram. Soc. 25 (2005) 293–300, http://dx.doi.org/10.1016/j.jeurceramsoc.2004.03.017.

[9] F. Güngör, I. Işık, E. Gungor, E. Gultekin, Usage of ZnO containing wastes in the sanitaryware bodies, J. Aust. Ceram. Soc. 55 (2019), http://dx.doi.org/10.1007/s41779-018-00300-8.

[10] M. Aksel, Ö. Kesmez, A. Yavaş, M.D. Bilgin, Titaniumdioxide mediated sonophotodynamic therapy against prostate cancer, J. Photochem. Photobiol. B: Biol. 225 (2021) 112333, http://dx.doi.org/10.1016/j.jphotobiol.2021.112333.

[11] K. Tekintas, Ö. Kesmez, O. Bekircan, E.T. Saka, Preparation, characterization and photocatalytic activity of novel 1,2,4-triazole based Cu(II) and Zn(II) phthalocyanines modified TiO_2 nanoparticles, J. Mol. Struct. 1248 (2022) 131405, http://dx.doi.org/10.1016/j.molstruc.2021.131405.

[12] Ö. Kesmez, Preparation of hybrid nanocomposite coatings via sol–gel method for hydrophobic and self-cleaning properties, J. Mol. Struct. 1205 (2020) 127572, http://dx.doi.org/10.1016/j.molstruc.2019.127572.

[13] A. Morfino, J. Gediga, K. Harlow, B. Mazzanti, Life cycle assessment comparison between zircon and alumina sand applied to ceramic tiles, Clean. Eng. Technol. 6 (2022) 100359, http://dx.doi.org/10.1016/j.clet.2021.100359.

[14] M. Dondi, G. Guarini, C. Melandri, M. Raimondo, C. Zanelli, Resistance to impact of porcelain stoneware tiles, Ceram. Int. 42 (2016) 5731–5736, http://dx.doi.org/10.1016/j.ceramint.2015.12.104.

[15] EN ISO 10545-3, Ceramic tiles — Part 3: Determination of water absorption, apparent porosity, apparent relative density and bulk density, International Standard Organization (2018).
[16] I.S. Vilarinho, E. Filippi, M.P. Seabra, Development of eco-ceramic wall tiles with bio-$CaCO_3$ from eggshells waste, Open Ceram. 9 (2022) 100220, http://dx.doi.org/10.1016/j.oceram.2022.100220.
[17] P.d.O. Piccolo, A. Zaccaron, L.B. Teixeira, E.G. de Moraes, O.R.K. Montedo, A.P.N. de Oliveira, Development of translucent ceramic tiles from modified porcelain stoneware tile paste, J. Build. Eng. 45 (2022) 103543, http://dx.doi.org/10.1016/j.jobe.2021.103543.
[18] M. Paganelli, Using the optical dilatometer to determine sintering behavior, Am. Ceram. Soc. Bull. 81 (2002) 25–30.
[19] N. Tamsu Selli, Relationship between microstructure and the impact resistance of porcelain stoneware tiles, Boletín de La Sociedad Española de Cerámica y Vidrio (2020), http://dx.doi.org/10.1016/j.bsecv.2020.10.001.
[20] R. Toro, M. Diab, T. De caro, M. Al-Shemy, A. Adel, D. Caschera, Study of the effect of titanium dioxide hydrosol on the photocatalytic and mechanical properties of paper sheets, Materials 13 (2020) 1326, http://dx.doi.org/10.3390/ma13061326.
[21] L. Chougala, M. Yatnatti, R. Linganagoudar, R. Kamble, J. Kadadevarmath, A simple approach on synthesis of TiO_2 nanoparticles and its application in dye sensitized solar cells, J. Nano- and Electron. Phys. 9 (2017) 4001–4005, http://dx.doi.org/10.21272/jnep.9(4).04005.
[22] O. Hussein, M. Alghalayini, S.J. Dillon, F. Abdeljawad, Unraveling the role of grain boundary anisotropy in sintering: implications for nanoscale manufacturing, ACS Appl. Nano Mater. 4 (2021) 8039–8049, http://dx.doi.org/10.1021/acsanm.1c01322.
[23] D.A. Alonso-De la Garza, E.A. Rodríguez, J.E. Contreras, J.F. López-Perales, L. Díaz-Tato, J.J. Ruiz-Valdés, et al., Effect of nano-TiO_2 content on the mechano-physical properties of electro-technical porcelain, Mater. Chem. Phys. 254 (2020) 123469, http://dx.doi.org/10.1016/j.matchemphys.2020.123469.
[24] A. Lee Kwan Yee, M. Razali, M.A.M. Ismail, I.N. Yusoff, S.K. Nagendran, Z. Zainal, et al., Preliminary analysis of rock mass weathering grade using image analysis of CIELAB color space with the validation of schmidt hammer: a case study, Phys. Chem. Earth A/B/C (2022) 103291, http://dx.doi.org/10.1016/j.pce.2022.103291.
[25] J. Yang, J. Wu, P. Rao, C. Fei, D. Chen, The influence of nanosized leucite on dental porcelain properties, Key Eng. Mater. 280–283 (2005) 1605–1608, http://dx.doi.org/10.4028/www.scientific.net/KEM.280-283.1605.
[26] F. Belnou, D. Goeuriot, P. Goeuriot, F. Valdivieso, Nanosized alumina from boehmite additions in alumina porcelain: 1. Effect on reactivity and mullitisation, Ceram. Int. 30 (2004) 883–892, http://dx.doi.org/10.1016/j.ceramint.2003.10.009.
[27] M. Bakhtierkhalzi, M. Wahedul Islam, M. Suzauddin, M. Nurul Islam, A. Al Mahmood, Effect of TiO_2 as sintering additive on microstructural, physical, and mechanical properties of CeO_2 doped zirconia toughened alumina ceramic composite, Ceram. Int. 49 (2023) 6666–6670, http://dx.doi.org/10.1016/j.ceramint.2022.10.282.
[28] X. Zhang, H. Zeng, X. Wang, W. Li, L. Hu, S. Chen, Effect of TiO_2 on crystallization and mechanical properties of $MgO–Al_2O_3–SiO_2$ glasses containing P_2O_5, Ceram. Int. 49 (2023) 12499–12507, http://dx.doi.org/10.1016/j.ceramint.2022.12.110.
[29] H.-N. Kuo, J.-H. Chou, T.-K. Liu, Microstructure and mechanical properties of microwave sintered ZrO_2 bioceramics with TiO_2 addition, Appl. Bionics Biomech. 2016 (2016) 1–7, http://dx.doi.org/10.1155/2016/2458685.